

Anisotropic magnetic properties and crystal electric field studies on CePd_2Ge_2 single crystal

Arvind Maurya, R. Kulkarni, S. K. Dhar and A. Thamizhavel*

Department of Condensed Matter Physics and Materials Science, Tata Institute of Fundamental Research, Homi Bhabha Road, Colaba, Mumbai 400 005, India

E-mail: *thamizh@tifr.res.in

Abstract.

The anisotropic magnetic properties of the antiferromagnetic compound CePd_2Ge_2 , crystallizing in the tetragonal crystal structure have been investigated in detail on a single crystal grown by Czochralski method. From the electrical transport, magnetization and heat capacity data, the Néel temperature is confirmed to be 5.1 K. Anisotropic behaviour of magnetization and resistivity is observed along the two principal crystallographic directions viz., [100] and [001]. The isothermal magnetization measured in the magnetically ordered state at 2 K exhibits a spin re-orientation at 13.5 T for field applied along [100] direction, whereas the magnetization was linear along the [001] direction attaining a value of $0.94 \mu_B/\text{Ce}$ at 14 T. The reduced value of the magnetization is attributed to the crystalline electric field (CEF) effects. A sharp jump in the specific heat at the magnetic ordering temperature is observed. After subtracting the phononic contribution, the jump in the heat capacity amounts to 12.5 J/K mol which is the expected value for a spin $\frac{1}{2}$ system. From the CEF analysis of the magnetization data the excited crystal field split energy levels were estimated to be at 120 K and 230 K respectively, which quantitatively explain the observed Schottky anomaly in the heat capacity. A magnetic phase diagram has been constructed based on the field dependence of magnetic susceptibility and the heat capacity data.

PACS numbers: 81.10.-h, 71.27.+a, 71.70.Ch, 75.10.Dg, 75.50.Ee

Submitted to: *J. Phys.: Condens. Matter*

1. Introduction

One of the most widely investigated topics in the field of condensed matter physics is the magnetism exhibited by Ce-based intermetallic compounds. In some Ce compounds the $4f$ level lies in close proximity to the Fermi level, enhancing the interaction between the conduction electrons and the f electron leading to Kondo effect which screens the $4f$ derived magnetic moment. The competition between the on-site Kondo effect with an energy scale $T_K \approx \exp(-1/[JN(E_F)])$ and the inter-site Ruderman-Kittel-Kasuya-Yosida (RKKY) magnetic interaction with an energy scale $T_{RKKY} \approx [J^2N(E_F)]$, where J is the exchange coupling between the local moment and the conduction electrons and $N(E_F)$ is the density of states at the Fermi level E_F , leads to various diverse ground states like magnetic ordering, valence instability, heavy fermion nature, unconventional superconductivity etc.; hence Ce based intermetallic compounds have been widely investigated for several decades. The CeT_2X_2 compounds, where T is a transition metal and X is Si or Ge, crystallizing in the very well known $ThCr_2Si_2$ - type body centered tetragonal crystal structure, have been particularly useful in this regard. For example, heavy-fermion superconductivity is observed in $CeCu_2Si_2$ [1], pressure induced superconductivity in $CePd_2Si_2$ [2], $CeRh_2Si_2$ [3, 4], $CeCu_2Ge_2$ [5], unconventional metamagnetism is observed in $CeRu_2Si_2$ [6]. The pressure induced superconductor $CePd_2Si_2$ has been investigated in greater detail on a single crystal by Van Dijk *et al* [7]. From the anisotropic magnetic studies, they observed a change in the easy axis direction from a -axis to c -axis at around 50 K. The reduced moment and a relatively large Sommerfeld coefficient γ in $CePd_2Si_2$ was attributed to Kondo effect with a strong spin fluctuation. The neutron diffraction experiments both on polycrystalline sample and single crystalline sample confirmed the antiferromagnetic ordering with the spins pointing along the $[110]$ direction [8, 7]. On the other hand, the magnetic properties of iso-electronic $CePd_2Ge_2$ have been investigated only on polycrystalline samples [9, 10, 11, 12]. Besnus *et al* [9] reported the magnetic and thermal properties of $CePd_2Ge_2$ which orders antiferromagnetically at $T_N = 5.1$ K. They estimated the crystal field parameters from the magnetic susceptibility and from the Schottky heat capacity and inferred the crystal field split energy levels to be located at 0, 110 and 220 K corresponding to the three doublets. The magnetic structure of $CePd_2Ge_2$ was determined by Feyerherm *et al* and they found that the magnetic moment points along the $[110]$ direction [10] similar to the case of $CePd_2Si_2$. Furthermore, they attributed the reduced ordered moment of $CePd_2Ge_2$ not due to Kondo effect but due to the CEF and the anisotropic exchange interaction [10]. The effect of chemical pressure by substituting Ni in place of Pd resulted in a decrease of T_N [12] whereas the hydrostatic pressure studies on resistivity measurement revealed that the T_N increases with increasing pressure up to values as high as 10 GPa [11, 13]. In continuation of our successful efforts in growing the single crystals and investigating the anisotropic magnetic properties of CeT_2Ge_2 type compounds (where T is a transition metal) like $CeAg_2Ge_2$ [14], $CeAu_2Ge_2$ [15] and $CeCu_2Ge_2$ [16], here we report on the anisotropic magnetic properties of $CePd_2Ge_2$

single crystal by measuring the transport and magnetic properties. CEF analysis has been performed on the magnetic susceptibility and heat capacity data to estimate the crystal field level splitting.

2. Experiment

The single crystal of CePd₂Ge₂ was grown by Czochralski crystal pulling method in a tetra-arc furnace. The starting materials of Ce (99.9% purity), Pd (99.99%) and Ge (99.9999%) were taken in the stoichiometric ratio for a total mass of about 10-11 g. The sample was remelted 4 times to ensure proper homogeneity in a water cooled copper hearth. A polycrystalline tungsten rod was used as a seed and the crystal was pulled out of the melt at a rate of 10 mm/hr. The pulled ingot was then subjected to powder x-ray diffraction (XRD), using a PANalytical x-ray diffractometer with monochromatic Cu-K_α radiation, to check the phase purity. The orientation of the crystal was done by back reflection Laue method. The dc magnetic susceptibility and the magnetization measurements were performed in the temperature range 1.8-300 K using a superconducting quantum interference device (SQUID) and vibrating sample magnetometer (VSM). The electrical resistivity was measured down to 1.9 K in a home made set up. The heat capacity was measured using a Quantum Design physical property measurement system (PPMS); we have also used the dilution insert of Quantum Design to measure the heat capacity down to 50 mK and in applied magnetic fields as high as 14 T.

3. Results

3.1. X-ray diffraction

To confirm the phase purity of CePd₂Ge₂ a small portion of the crystal was subjected to powder x-ray diffraction. The XRD revealed a clear pattern without any impurity peaks suggesting the phase purity of the grown crystal. A Le-Bail fit was performed on the x-ray diffraction pattern and the lattice constants were estimated to be $a = 4.337 \text{ \AA}$ and $c = 10.051 \text{ \AA}$ which are in agreement with the previously reported values [17]. The composition of the crystal was further confirmed by energy dispersive analysis by x-ray (EDAX). In order to study the anisotropic physical properties, the grown single crystal was cut along the principal crystallographic directions viz., [100] and [001]. This was accomplished by performing a back-reflection Laue. The Laue diffraction patterns corresponding to the (100) and (001) planes are shown in Fig. 1. Well defined Laue diffraction spots together with the tetragonal symmetry pattern confirmed the good quality of the grown crystal. The crystal was then cut along the principal crystallographic direction using a spark erosion cutting machine for the measurement of resistivity, susceptibility and heat capacity.

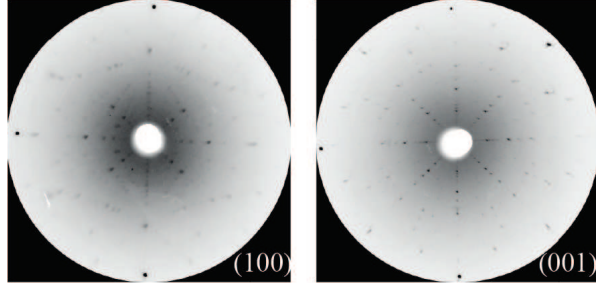


Figure 1. (Color online) Laue diffraction pattern of CePd_2Ge_2 single crystal corresponding to the (100) and (001) planes.

3.2. Magnetization

The temperature dependence of magnetic susceptibility of CePd_2Ge_2 is shown in the main panel of Fig. 2(a), measured in an applied magnetic field of 0.1 T from 1.8 K to 300 K. The magnetic susceptibility for $H \parallel [001]$ direction is larger than for $H \parallel [100]$, both in the paramagnetic and in the magnetically ordered state, reflecting the anisotropy. For temperatures fairly higher than T_N the susceptibility shows Curie-Weiss like behaviour. The low temperature part of the magnetic susceptibility along the three crystallographic directions [100], [110] and [001] is shown in the left inset of Fig. 2(a). For field parallel to [100] direction, the susceptibility exhibits a clear cusp at 5.1 K indicating the antiferromagnetic transition at this temperature. On the other hand, the magnetic susceptibility shows a kink followed by an increase at 5.1 K for the [001] direction. Similar behaviour is also observed for the isostructural CePd_2Si_2 compound [7]. Typically in a collinear two sublattice antiferromagnet, when the field is applied parallel to the moment direction, the susceptibility will apparently decrease to zero at $T \rightarrow 0$ and for fields orthogonal to the moment direction the susceptibility will remain almost constant, below T_N . The increase in the susceptibility along [001] direction and a relatively large drop in the susceptibility below ($T_N =$) 5.1 K in the ab -plane suggests that [001] direction may be the hard axis of magnetization and the magnetic moment must be lying in the ab -plane as predicted by neutron diffraction experiments on polycrystalline samples [10]. From our susceptibility measurement it is obvious that the magnetic susceptibility falls more rapidly for $H \parallel [100]$ direction, than along the other two directions, suggesting [100] is the easy axis of magnetization. The inverse magnetic susceptibility of CePd_2Ge_2 is shown in the right inset of Fig. 2. At high temperatures the inverse susceptibility is linear and at low temperature there is a deviation from this linearity. This deviation is attributed to the crystalline electric field effect which is discussed later. The high temperature part of the magnetic susceptibility is fitted to the Curie-Weiss law, $\chi = \frac{C}{T - \theta_p}$, where C is the Curie constant and θ_p is the paramagnetic Weiss temperature. We obtain $\theta_p = -47$ K and $\mu_{\text{eff}} = 2.65 \mu_B/\text{Ce}$, $\theta_p = -46$ K and $\mu_{\text{eff}} = 2.64 \mu_B/\text{Ce}$ and $\theta_p = -5$ K and $\mu_{\text{eff}} = 2.74 \mu_B/\text{Ce}$ for $H \parallel [100]$, [110] and [001] directions, respectively. The negative sign of θ_p suggests the antiferromagnetic ordering and the effective magnetic moment is close to the free ion value of Ce^{3+} .

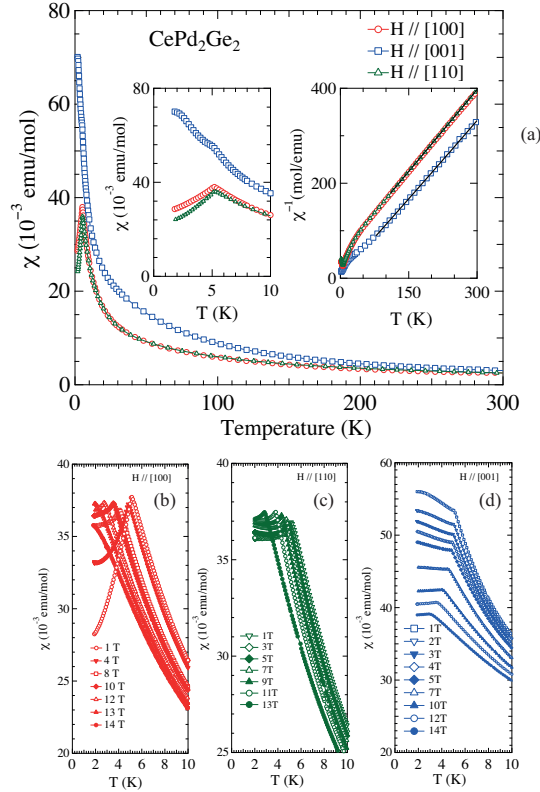


Figure 2. (Color online) (a) Temperature dependence of magnetic susceptibility of $CePd_2Ge_2$ for magnetic field parallel to [100], [110] and [001] directions. The left inset shows the low temperature part where the magnetic ordering is seen clearly. The right inset shows the inverse magnetic susceptibility of $CePd_2Ge_2$, the solid lines are fit to the Curie-Weiss law. (b), (c) & (d) Low temperature part of the magnetic susceptibility in various applied magnetic fields along [100], [110] and [001] directions, respectively.

We also measured the susceptibility in various applied fields along the two principal crystallographic directions. It is evident from Fig. 2(b) that for fields parallel to [100] direction the antiferromagnetic transition shifts to lower temperatures. For magnetic fields greater than 12.5 T, the susceptibility does not show any clear evidence of magnetic ordering down to 1.8 K. Apparently the magnetic transition become very broad at high fields around 14 T. On the other hand a clear anomaly persists at low temperature pertaining to the magnetic ordering even at fields as high as 14 T along the [110] and [001] direction. This supports the claim that [001]-axis is the hard axis of magnetization.

The anisotropic magnetic behaviour of $CePd_2Ge_2$ was further investigated by performing isothermal magnetization measurements $M(H)$ at a few selected temperatures. The main panel of Fig.3 shows the magnetization of $CePd_2Ge_2$ at 2 K along the two principal crystallographic directions. For $H \parallel [100]$, the magnetization initially increases linearly with the field followed by a small change in the slope at 2.4 T, and then it increases almost linearly up to 13 T at which point there is another clear change of slope indicating the spin reorientation at these two fields. On the other hand the magnetization for $H \parallel [001]$ direction simply increases with the increase in field

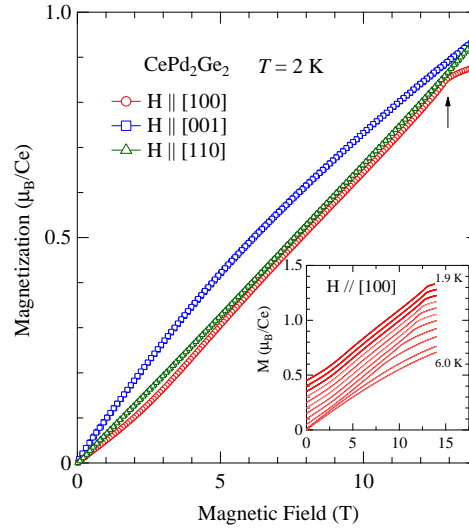


Figure 3. (Color online) Isothermal magnetization of $CePd_2Ge_2$ measured at $T = 2$ K for $H \parallel [100]$ and $[001]$ directions. The inset shows the isothermal magnetization measured at various fixed temperatures for $H \parallel [100]$. The magnetization curves have been shifted up for clarity. The plots from the top are for temperatures 1.9, 2.2, 2.4, 2.6, 2.8, 3, 3.5, 4, 5 and 6 K.

with a positive curvature and does not exhibit any evidence of spin re-orientation. The magnetization along $[110]$ direction almost overlaps with that of $[100]$ direction, however the spin reorientation observed along $[100]$ direction is not seen. The magnetization reaches a value of $0.88 \mu_B/Ce$ and $0.94 \mu_B/Ce$ at 14 T along $[100]$ and $[001]$ respectively. These values of magnetization are much smaller than the theoretical value of $g_J J$ ($=\frac{6}{7} \times \frac{5}{2}$), $2.14 \mu_B/Ce$. The inset of Fig. 3 shows the $M(H)$ measured at various temperatures for $H \parallel [100]$. It is evident that the spin reorientation occurring at 13.4 T at 2 K decreases to lower values as the temperature increases. Close to the magnetic ordering temperature 5 K, the spin re-orientation is not discernible.

3.3. Electrical Resistivity

Figure 4 shows the electrical resistivity of $CePd_2Ge_2$ measured in the temperature range from 1.8 to 300 K for current parallel to the two principal crystallographic directions, respectively. There is a significant anisotropy in the electrical resistivity reflecting the tetragonal symmetry of the crystal and most likely an anisotropic Fermi surface. The low temperature part of the electrical resistivity is shown in the inset of Fig. 4. The sudden drop in the electrical resistivity at 5.1 K is attributed to the antiferromagnetic ordering, which occurs due to the reduction in the spin-disorder scattering. As the sample is cooled below 300 K the resistivity decreases typical of a metallic sample. The absolute value of electrical resistivity at 300 K is $77 \mu\Omega \cdot cm$ and $32 \mu\Omega \cdot cm$ for $J \parallel [100]$ and $[001]$ respectively which decrease to $17 \mu\Omega \cdot cm$ and $8 \mu\Omega \cdot cm$ at 1.8 K, respectively. It is to be mentioned here that in $CePd_2Si_2$ also the electrical resistivity is

larger along [100] direction than that in the [001] direction [7]. However, unlike the case of $CePd_2Si_2$, where a clear $-\ln(T)$ behaviour is seen below 50 K, no such anomaly is observed in $CePd_2Ge_2$ this may be attributed to the larger unit cell volume of $CePd_2Si_2$, which does not favour Kondo effect. A broad hump centered around 100 K is observed

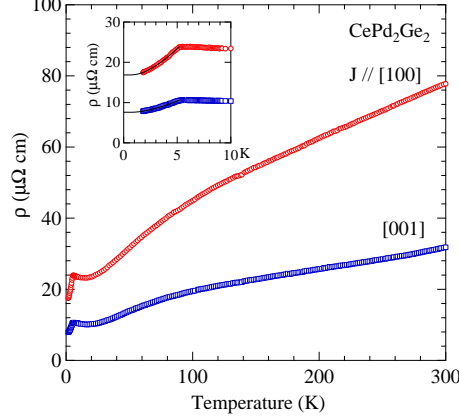


Figure 4. (Color online) Temperature dependence of electrical resistivity of $CePd_2Ge_2$ for current parallel to the two principal crystallographic directions. The inset shows the low temperature part of the resistivity and the solid lines are the fits to antiferromagnetic spin-wave gap expression (see text).

along both the directions which is attributed to the crystal field effect. Assuming that the excitation of spin waves is governed by the dispersion relation [18],

$$\epsilon_k = \sqrt{\Delta^2 + Dk^2}, \quad (1)$$

where ϵ_k is the energy of the excitations, Δ is the gap in the spin-wave spectrum and D is the spin-wave stiffness, the electrical resistivity in the ordered state is given by [18],

$$\rho(T) = \rho_0 + \rho_{AF}\Delta^2\sqrt{\frac{T}{\Delta}}e^{-\frac{\Delta}{T}}\left[1 + \frac{2}{3}\left(\frac{T}{\Delta}\right) + \frac{2}{15}\left(\frac{T}{\Delta}\right)^2\right], \quad (2)$$

where the coefficient ρ_{AF} is proportional to $\frac{1}{D^{3/2}}$ and ρ_0 is the residual resistivity which is temperature independent. Eq. 2 was fitted to the low temperature electrical resistivity data of $CePd_2Ge_2$ below T_N and the obtained fitting parameters are $\rho_0 = 16.873 \mu\Omega\cdot\text{cm}$, $\rho_{AF} = 0.399 \mu\Omega\cdot\text{cm}/\text{K}^2$ and $\Delta = 3.962 \text{ K}$ for $J \parallel [100]$ and $\rho_0 = 7.592 \mu\Omega\cdot\text{cm}$, $\rho_{AF} = 0.172 \mu\Omega\cdot\text{cm}/\text{K}^2$ and $\Delta = 3.814 \text{ K}$ for $J \parallel [001]$. Although the above equation is valid for $T \ll \Delta$, it provides a good fit to our experimental data in the magnetically ordered state right upto T_N . The spin-wave gap is almost the same for both the crystallographic directions and it is comparable to T_N as observed in other antiferromagnet Ce compounds [19, 20].

3.4. Heat Capacity

Figure 5 shows the temperature dependence of the heat capacity C_p of $CePd_2Ge_2$ measured in the temperature range 0.05 to 80 K. Also shown in the main panel of Fig. 5 is the specific heat capacity of the non-magnetic analogue $LaPd_2Ge_2$ in the temperature range from 1.8 to 80 K. The observed heat capacity of $LaPd_2Ge_2$ is typical

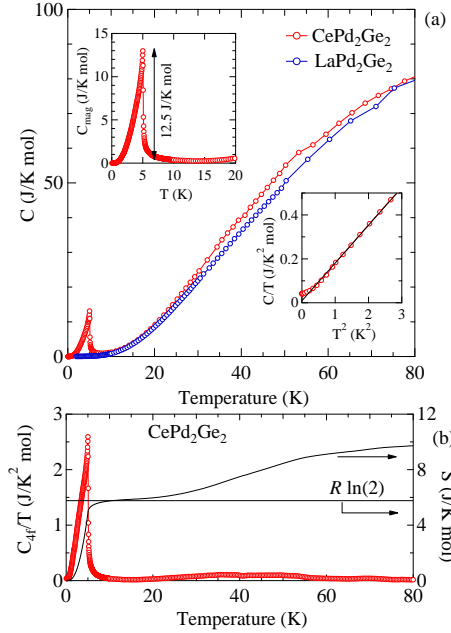


Figure 5. (Color online) (a) Temperature dependence of the specific heat capacity of $CePd_2Ge_2$ measured in the temperature range from 0.05 to 80 K and $LaPd_2Ge_2$ measured in the temperature range from 1.8 to 80 K. The top inset shows the magnetic part of heat capacity and the lower inset shows the C/T vs. T^2 plot of $CePd_2Ge_2$. (b) C_{4f}/T vs. T of $CePd_2Ge_2$. The calculated entropy is plotted in the right axis.

for a non-magnetic reference compound. The low temperature part of the heat capacity of $LaPd_2Ge_2$ was fitted to the expression $C/T = \gamma + \beta T^2$ to obtain the electronic specific heat coefficient γ and the lattice contribution β . The γ and β were estimated to be 8.03 mJ/K²·mol and 0.427 mJ/K⁴mol. From the β value one can estimate the Debye temperature Θ_D as 283 K, which is typical of most of the La-based compounds. The specific heat capacity of $CePd_2Ge_2$ shows a huge jump at 5.1 K thus confirming the bulk magnetic ordering. The C_p of $CePd_2Ge_2$ is higher than the non-magnetic reference compound in the temperature range investigated in the present work. An estimate of the Sommerfeld coefficient γ for $CePd_2Ge_2$ was obtained by the same method as employed for $LaPd_2Ge_2$ from the data below 1.7 K as shown in the lower inset of Fig. 5. The γ value thus obtained is 9.17 mJ/K² mol which is close to that of $LaPd_2Ge_2$, thus indicating that the strength of the hybridization between the 4*f* electron and the conduction electrons in $CePd_2Ge_2$ is very weak. The 4*f* contribution to the heat capacity C_{4f} was obtained by subtracting the specific heat of $LaPd_2Ge_2$ from that of $CePd_2Ge_2$.

The top inset in Fig. 5(a) shows the C_{4f} , where the jump in the heat capacity at T_N amounts to 12.5 J/K mol. In the mean field approximation the discontinuity in the magnetic part of the heat capacity for a spin $S(= \frac{1}{2})$ system is given by [21],

$$\Delta C_{\text{mag}}(T_N) = 2.5R \left[\frac{(2S + 1)^2 - 1}{(2S + 1)^2 + 1} \right], \quad (3)$$

where R is the gas constant. The jump in the heat capacity observed in $CePd_2Ge_2$ exactly matches with the theoretical model. The estimated magnetic entropy obtained by integrating C_{4f}/T is shown in Fig. 5(b). The entropy reaches 90% of $R\ln(2)$ at the ordering temperature and recovers the full value for a doublet ($R\ln(2)$) at 10 K thus indicating a doublet ground state well separated from the first excited state. Above T_N the entropy increases gradually and reaches $R \ln 4$ for temperatures greater than 100 K. This roughly gives the estimate of the first excited state of the crystal field split level which is discussed in the next section.

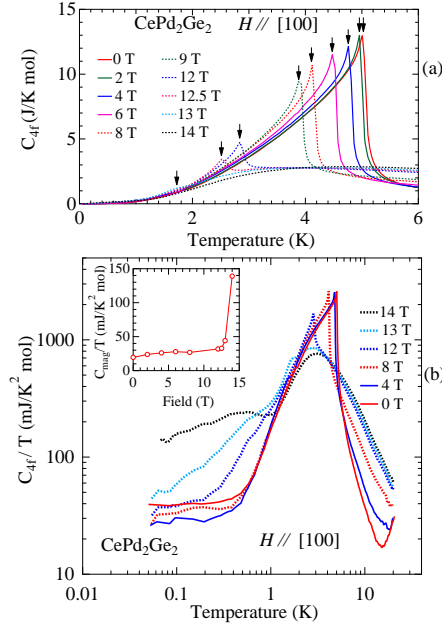


Figure 6. (Color) (a) Magnetic part of the heat capacity ($C_{\text{mag}}(T)$) in the temperature range from 0.05 to 6 K of $CePd_2Ge_2$, in various applied magnetic fields along the [100] direction. The arrows indicate the antiferromagnetic ordering. (b) Log-Log plot of C_{mag}/T of $CePd_2Ge_2$ in various applied magnetic fields in the temperature range from 0.05 to 20 K. The inset shows the value of C_{mag}/T at 0.05 K.

Figure 6 shows the magnetic part of the heat capacity measured in various applied magnetic fields, up to 14 T with $H \parallel [100]$ direction. It is evident that the antiferromagnetic transition shifts to lower temperature, typical for an antiferromagnetic system. The shift to lower temperatures with the field corresponds well with the data depicted in Fig. 2(b). The peak due to antiferromagnetic order is discernible up to fields as high as 13 T, where T_N has decreased down to 1.7 K. For an applied field of 14 T the peak is not seen down to 0.05 K; instead a broad hump is observed. From the log-log

plot of C_{mag}/T , one can see from Fig. 6(b) that for fields greater than 12 T, the curves fall almost on a single trace in the paramagnetic region. The inset of Fig. 6 shows that C_{mag}/T value close to 0.05 K increases rapidly beyond 13 T. Similar type of behaviour is seen in $CeAuSb_2$ ($T_N=6$ K) which exhibits field induced quantum critical point at 5.4 T and C_{mag}/T increases rapidly in the vicinity of critical point and shows a peak at the critical field [22].

4. Discussion

From the magnetic susceptibility, electrical resistivity and heat capacity measurements it is inferred that the single crystal of $CePd_2Ge_2$ undergoes an antiferromagnetic ordering at $T_N = 5.1$ K which is coincident with the T_N of polycrystalline samples reported by Besnus *et al.* [9, 11]. The field dependence of magnetic susceptibility and the heat capacity on single crystalline sample enabled us to construct a magnetic phase diagram

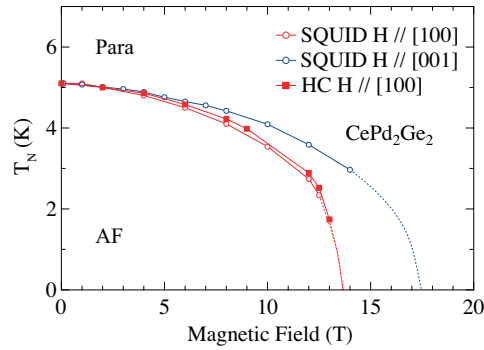


Figure 7. (Color online) Magnetic phase diagram of $CePd_2Ge_2$. The dashed lines are guide to the eyes.

which is shown in Fig. 7. The Néel temperature above 6 T decreases much faster along [100] than that of [110] and [001] directions. This suggests that [001] direction is the hard axis of magnetization. Furthermore, the magnetization reaches only $0.88 \mu_B/Ce$ and $0.94 \mu_B/Ce$ for $H \parallel [100]$ and [001] directions, respectively at 14 T. These values are consistent with the neutron diffraction results on a polycrystalline sample where the ordered moment was reported to be $0.85 \mu_B/Ce$ at 1.8 K [10]. It is to be mentioned here that in the isostructural $CePd_2Si_2$, the ordered moment is only $0.62 \mu_B/Ce$. This reduced value of moment in $CePd_2Si_2$ is attributed to the Kondo effect, where a $-\ln(T)$ behaviour is observed in the electrical resistivity and the jump in the heat capacity at the magnetic transition is lower, with the magnetic entropy amounting to $0.6 - 0.75 R \ln 2$ [23, 24]. Since no such behaviour is observed in $CePd_2Ge_2$ the reduced value of magnetization is mainly attributed to the crystal electric field effect.

We analysed the magnetic susceptibility and the heat capacity using the point charge CEF model. The Ce atoms in $CePd_2Ge_2$ occupy the $2a$ Wyckoff's position and possesses the D_{4h} tetragonal point symmetry. For tetragonal site symmetry, for $J = 5/2$, the $2J + 1$ 6-fold degenerate level splits into three doublets. To understand

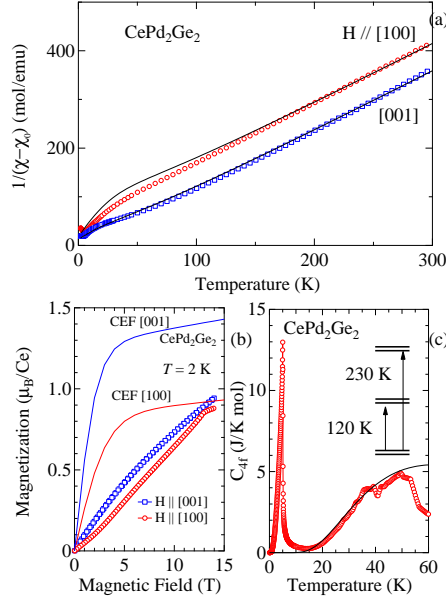


Figure 8. (Color online) (a) Inverse magnetic susceptibility of CePd_2Ge_2 . The solid line is based on the CEF calculation, (b) The isothermal magnetization data of CePd_2Ge_2 along with the magnetization calculated based on the CEF parameters (c) magnetic part of the specific heat capacity of CePd_2Ge_2 . The solid line is calculated Schottky heat capacity. The obtained energy levels are also shown.

the observed anisotropy in the magnetic susceptibility and to know the crystal field energy splitting, we have performed the crystal field analysis on these data. For this purpose in Fig. 8(a) we have plotted the susceptibility data as $1/(\chi - \chi_0)$, where χ_0 was estimated as -5.571×10^{-5} and 1.230×10^{-4} emu/mol for $H \parallel [100]$ and $[001]$ directions, respectively, so an effective magnetic moment of $2.54 \mu_B/\text{Ce}$ is obtained for temperature above 50 K. A similar approach was taken for CePt_3Si and CeAg_2Ge_2 while performing the CEF analysis of the susceptibility data [25, 26]. The CEF Hamiltonian for the tetragonal site symmetry is given by

$$\mathcal{H}_{\text{CEF}} = B_2^0 O_2^0 + B_4^0 O_4^0 + B_4^4 O_4^4 + B_6^0 O_6^0 + B_6^4 O_6^4, \quad (4)$$

where B_ℓ^m and O_ℓ^m are the CEF parameters and the Stevens operators, respectively [28, 29]. For Ce atom the O_6 Stevens operators are zero and hence the last two terms in the Hamiltonian are zero.

The magnetic susceptibility including the molecular field contribution λ_i is given by

$$\chi_i^{-1} = \chi_{\text{CEF}i}^{-1} - \lambda_i. \quad (5)$$

The expression for the magnetic susceptibility based on the CEF model is given in our previous report [27]. We have calculated the inverse magnetic susceptibility for field along the two principal crystallographic directions based on the above CEF model. By diagonalizing the CEF Hamiltonian the eigenvalues and eigenfunctions are

Table 1. CEF parameters, energy level schemes and the corresponding wave functions for $CePd_2Ge_2$.

CEF parameters						
B_2^0 (K)	B_4^0 (K)	B_4^4 (K)	λ_i (emu/mol) ⁻¹			
-4.18	-0.25	-3.75	$\lambda_{[100]} = -17$			
			$\lambda_{[001]} = -12$			
energy levels and wave functions						
E (K)	$ +5/2\rangle$	$ +3/2\rangle$	$ +1/2\rangle$	$ -1/2\rangle$	$ -3/2\rangle$	$ -5/2\rangle$
230	0.8603	0	0	0	0.5098	0
230	0	0.5098	0	0	0	0.8603
120	0	0	1	0	0	0
120	0	0	0	1	0	0
0	0	0.8603	0	0	0	-0.5098
0	-0.5098	0	0	0	0.8603	0

obtained. The eigenvalues corresponds to the energy levels. The solid lines in Fig. 8(a) are the calculated susceptibility with the unique values of the crystal field parameters given in Table 1. The negative value of the exchange field constant indicates the antiferromagnetic interaction between Ce moments. From the obtained eigenfunctions it is observed that there is a mixing of $|\pm \frac{5}{2}\rangle$ and $|\pm \frac{3}{2}\rangle$ wave functions in the ground and second excited state while the first excited state is composed mainly of $|\pm \frac{1}{2}\rangle$. These crystal field parameters reproduce the experimental susceptibility reasonably well and are in close agreement with the parameters estimated by Besnus *et al* [9] from the data obtained for a polycrystalline sample. The obtained energy levels are $\Delta_1 = 120$ K and $\Delta_2 = 230$ K. Figure 8(b) shows the isothermal magnetization plot of $CePd_2Ge_2$ measured at $T = 2$ K together with the calculated magnetization curves. Although the CEF calculated magnetization curves do not reproduce the experimental data, it should be noted here that the anisotropy in the magnetization along the [100] and [001] directions are clearly explained. $CePd_2Ge_2$ is one of the systems where the magnetization, in the ordered state, is larger for the axis which is perpendicular to the direction of the moment orientation [10]. Similar kind of behaviour is seen in $CeAgSb_2$ where the magnetization increases very rapidly along the hard axis direction [100], than along the easy axis direction [001] [30] and the ordered moment points along the [001] direction [31]. A detailed neutron diffraction study on single crystal will lead to a more comprehensive understanding of the magnetic structure of $CePd_2Ge_2$.

The magnetic part of the heat capacity of $CePd_2Ge_2$ obtained after subtracting the heat capacity of $LaPd_2Ge_2$, shown in Fig. 8(c) exhibits a broad peak above 40 K which is attributed to the Schottky type excitations between the CEF levels of the Ce^{3+} ions. The Schottky heat capacity for a 3 level system (a ground state and two excited states)

is given by the following expression

$$C_{\text{Sch}} = \left[\frac{R}{(k_{\text{B}}T)^2} \frac{e^{(\Delta_1+\Delta_2)/k_{\text{B}}T} [-2\Delta_1\Delta_2 + \Delta_2^2(1 + e^{\Delta_1/k_{\text{B}}T}) + \Delta_1^2(1 + e^{\Delta_2/k_{\text{B}}T})]}{(e^{\Delta_1/k_{\text{B}}T} + e^{\Delta_2/k_{\text{B}}T} + e^{(\Delta_1+\Delta_2)/k_{\text{B}}T})^2} \right] \quad (6)$$

where R is the gas constant and Δ_1 and Δ_2 are the crystal field split excited energy levels. Having found the energy spacing for the first and the second excited doublets from the magnetic susceptibility, we have used the same energy values $\Delta_1 = 120$ K and $\Delta_2 = 230$ K in Eqn. 6 and found that it explains the observed Schottky anomaly. The solid line in Fig. 8(c) shows the calculated Schottky heat capacity, thus validating our crystal field splitting estimation from the susceptibility data. The discrepancy above 50 K may be attributed to the difference in the phonon spectra of LaPd₂Ge₂ and CePd₂Ge₂ at higher temperatures.

The application of magnetic field shifts the antiferromagnetic ordering to lower temperatures which is more prominent along the [100] direction than along the [001] direction, as evident from the magnetic phase diagram shown in Fig. 7. The low value of the Sommerfeld coefficient γ (9.2 mJ/K²·mol) in CePd₂Ge₂ which is comparable to that of LaPd₂Ge₂ indicates that the hybridization between the conduction electron and the f electron is weak and the f electrons are highly localized here. Furthermore, it is evident from the inset of Fig. 6(b) that the C_{mag}/T increases to a large value in the magnetic field when the antiferromagnetic ordering vanishes, and is attributed to the spin fluctuations. The enhancement in the C_{mag}/T value, when the antiferromagnetic ordering vanishes due to the application of magnetic field is also observed in CeAuSb₂, which shows a field induced quantum critical point [22]. It will be interesting to see the effect of magnetic field on the electrical resistivity of CePd₂Ge₂, down to very low temperature, which is planned for the future.

5. Conclusion

The anisotropic magnetic properties of CePd₂Ge₂ have been investigated by growing a single crystal, in a tetra-arc furnace. The phase purity and the crystal composition was confirmed by x-ray diffraction and EDAX. The transport and magnetic properties have revealed large anisotropy along the two principal crystallographic directions viz., [100] and [001], reflecting the tetragonal crystal structure. The antiferromagnetic order is confirmed as $T_{\text{N}} = 5.1$ K. The electrical resistivity in the ordered state can be well explained by the spin-wave gap model. The Néel temperature was found to decrease with increasing field, as expected for a typical antiferromagnet system. For fields greater than 13 T, the magnetic ordering was found to vanish. Our crystal field calculation clearly explains the anisotropy in the magnetic susceptibility and the magnetization and the energy level thus obtained for the first and second excited state was found to be 120 K and 230 K. These energy levels clearly explained the Schottky anomaly in the magnetic part of the heat capacity. The jump in the magnetic part of the heat capacity was found to 12.5 J/K mol as expected by the mean field model for a spin 1/2 system. There was no signature of Kondo effect and the magnetic ordering in this system is

believed to be purely Ruderman-Kittel-Kasuya-Yosida (RKKY) type interaction. One of the interesting findings is that although the magnetization is larger along the [001] direction as observed experimentally and supported by the CEF calculation, the moment direction is orthogonal to it, oriented in the ab -plane.

References

- [1] Steglich F, Aarts J, Bredl C D, Lieke W, Meschede D, Franz W and Schafer H 1979 *Phys. Rev. Lett.* **43** 1892
- [2] Sheikin I, Steep E, Braithwite D, Brison J P, Raymond S, Jaccard D and Flouquet J 2001 *J. Low Temp. Phys.* **122** 591
- [3] Movshovich R, Graf T, Mandrus D, Thompson J D, Smith J L and Fisk Z 1996 *Phys. Rev. B* **53** 8241
- [4] Araki S, Nakashima M, settai R, Kobayashi T C and Ōnuki Y. 2002 *J. Phys.: Condens. Matter* **14** L377
- [5] Jaccard D, Behnia K and Sierro J. 1992 *Phys. Lett. A* **163** 475
- [6] Haen P, Flouquet J, Labpierre F, Lejay P and Remenyi G 1987 *J. Low Temp. Phys.* **67** 391
- [7] van Dijk N H, FäK B, Charvolin T, Lejay P and Mignot J M 2000 *Phys. Rev. B* **61** 8922
- [8] Grier B H, Lawrence J M, Murgai V and Parks R D 1984 *Phys. Rev. B* **29** 2664
- [9] Besnus M J, Essaihi A, Fischer G, Hamdaoui N and Meyer A 1992 *J. Magn. Magn. Mater.* **104-107**, 1387
- [10] Feyerherm R, Becker B, Collins M F, Mydosh J, Nieuwenhuys G J and Ramakrishnan S 1998 *Physica B* **241-243** 643.
- [11] Oomi G, Uwatoko Y, Sampathkumaran E V and Ishikawa M 1996 *Physica B* **223 & 224** 307
- [12] Fukuhara T, Akamaru S, Kuway T, Sakurai J and Maezawa K 1998 *J. Phys. Soc. of Jpn.* **67** 2084
- [13] Wilhelm H and Jaccard D 2002 *Phys. Rev. B* **66**, 064428
- [14] Thamizhavel A, Kulkarni R and Dhar S K 2007 *Phys. Rev. B*, **75** 144426
- [15] Joshi D A, Nigam A K, Dhar S K and Thamizhavel A 2010 *J. Magn. Magn. Mater.*, **322** 3363
- [16] Singh D K, Thamizhavel A, Lynn J W, Dhar S, Rodriguez-Rivera J and Herman T 2011 *Sci. Rep.* **1** 117 DOI:10.1038/srep00117
- [17] Rossi D Marazza, R 1979 R Ferro, *J. Less-Common Met.* **66** P17
- [18] Fontes M B, Trochez J C, Giordanengo B Bud'ko, S L, Sanches D R, Baggio-Saitovitch E M and Cotinentino M A 1999 *Phys. Rev. B* **60** 6781
- [19] Pikul A P, Kaczorowski D, Plackowski T, Czopnik A, Michor H, Bauer E, Hilscher G, Rogl P and Grin Yu 2003 *Phys. Rev. B* **67** 224417
- [20] Szlawaska M and Kaczorowski D 2012 *Phys. Rev. B* **85**, 134423
- [21] Buschow K H J 2005 *Concise encyclopedia of magnetic and superconducting materials* 2nd Edition (Elsevier) p.710
- [22] Balicas L, Nakatsuji S, Lee H, Schlottmann P, Murphy T P and Fisk Z 2005 *Phys. Rev. B* **72** 064422
- [23] Dhar S K and Sampathkumaran E V 1987 *Phys. Lett. A* **121**, 454
- [24] Sheikin I, Wang Y, Bouquet F, Lejay P and Junod A 2002 *J. Phys.:Condens. Mater* **14**, L543
- [25] Takeuchi T, Hashimoto S, Yasuda T, Shishido H, Ueda T, Yamada M, Obiraki Y, Shiimoto M, Kohara H, Yamamoto T, Sugiyama K, Kindo K, Matsuda T D, Haga Y, Aoki Y, Sato H, Settai R and Ōnuki Y 2004 *J. Phys.: Condens. Matter* **16** L333
- [26] Thamizhavel A, Kulkarni R and Dhar S K 2007 *Phys. Rev. B* **75** 144426
- [27] Das P K, Kumar N, Kulkarni R and Thamizhavel A 2011 *Phys. Rev. B* **83**, 134416
- [28] Hutchings M T 1965 *Solid State Physics: Advances in Research and Applications* **Vol.16** ed F Seitz and B Turnbull (New York: Academic) p.227.
- [29] Stevens K W H 1952 *Proc. Phys. Soc. (London)* **Sect.A65** 209

- [30] Takeuchi T, Thamizhavel A, Okubo T, Yamada M, Nakamura N, Yamamoto T, Inada Y, Sugiyama K, Galatanu A, Yamamoto E, Kindo K, Ebihara T and Ōnuki Y 2003 *Phys. Rev. B* **67** 064403
- [31] Araki S, Metoki N, Galatanu A, Yamamoto E, Thamizhavel A and Ōnuki Y. 2003 *Phys. Rev. B* **68** 024408